

NEW CONSTRAINTS ON THE GALACTIC BAR

I. MINCHEV¹, J. NORDHAUS^{1,2} AND A. C. QUILLEN¹

Draft version November 7, 2018

ABSTRACT

Previous work has related the Galactic Bar to structure in the local stellar velocity distribution. Here we show that the Bar also influences the spatial gradients of the velocity vector via the Oort constants. By numerical integration of test-particles we simulate measurements of the Oort C value in a gravitational potential including the Galactic Bar. We account for the observed trend that C is increasingly negative for stars with higher velocity dispersion. By comparing measurements of C with our simulations we improve on previous models of the Bar, estimating that the Bar pattern speed is $\Omega_b/\Omega_0 = 1.87 \pm 0.04$, where Ω_0 is the local circular frequency, and the Bar angle lies within $20^\circ \leq \phi_0 \leq 45^\circ$. We find that the Galactic Bar affects measurements of the Oort constants A and B less than ~ 2 km/s/kpc for the hot stars.

Subject headings:

1. INTRODUCTION

The Galaxy is often modeled as an axisymmetric disk. With the ever increasing proper motion and radial velocity data, it is now apparent that nonaxisymmetric effects cannot be neglected (nonzero Oort constant C , Olling & Dehnen 2003, hereafter O&D; nonzero vertex deviation, Famaey et al. 2005; asymmetries in the local velocity distribution of stars, Dehnen 1998). It is still not clear, however, what the exact nature of the perturbing agent(s) in the Solar neighborhood (SN) is(are). Possible candidates are spiral density waves, a central Bar, and a triaxial halo.

Due to our position in the Galactic disk, the properties of the Milky Way Bar are hard to observe directly. Hence its parameters, such as orientation and pattern speed, have only been inferred indirectly from observations of the inner Galaxy (e.g., Blitz & Spergel 1991; Weinberg 1992).

However, the Bar has also been found to affect the local velocity distribution of stars. *HIPPARCOS* data revealed more clearly a stream of old disk stars with an asymmetric drift of about 45 km/s and a radial velocity $u < 0$, with u and v positive toward the Galactic center and in the direction of Galactic rotation, respectively. This agglomeration of stars has been dubbed the “Hercules” stream or the “ u -anomaly”. The numerical work of Dehnen (1999, 2000) and Fux (2001) has shown that this stream can be explained as the effect of the Milky Way Bar if the Sun is placed just outside the 2:1 Outer Lindblad Resonance (OLR). Using high-resolution spectra of nearby F and G dwarf stars, Bensby et al. (2007) have investigated the detailed abundance and age structure of the Hercules stream. Since this stream is composed of stars of different ages and metallicities pertinent to both thin and thick disks, they concluded that a dynamical effect, such as the influence of the Bar, is a more likely explanation than a dispersed cluster.

Assuming the Galactic Bar affects the shape of the distribution function of the old stellar population in the SN, an additional constraint on the Bar can be provided by considering the values derived for the Oort constant C . In other words, in addition to relating the dynamical influence of the Bar to the local velocity field, C provides a link to the gradients of the velocities as well. The study of O&D not only measured a non-zero C , implying the presence of non-circular motion in the SN, but also found that C is more negative for older and redder stars with a larger velocity dispersion. This is surprising as a hotter stellar population is expected to have averaged properties more nearly axisymmetric and hence, a reduced value of $|C|$ (e.g., Minchev & Quillen 2007; hereafter Paper I).

It is the aim of this letter to show it is indeed possible to explain the observationally deduced trend for C (O&D) by modeling the Milky Way as an exponential disk perturbed by a central Bar. By performing this exercise, we provide additional constraints on the Bar’s pattern speed. Models for the structure in the bulge of our galaxy are difficult to constrain because of the large numbers of degrees of freedom in Bar models. Thus future studies of structure in the Galactic Center will benefit from tighter constraints on the parameters describing the Bar, such as its pattern speed and angle with respect to the Sun.

2. THE OORT CONSTANTS

We can linearize the local velocity field (e.g., Paper I) about the LSR and write the mean radial velocity \bar{v}_d and longitudinal proper motion $\bar{\mu}_l$ as functions of the Galactic longitude l as

$$\begin{aligned} \frac{\bar{v}_d}{\bar{d}} &= K + A \sin(2l) + C \cos(2l) \\ \bar{\mu}_l &= B + A \cos(2l) - C \sin(2l) \end{aligned} \quad (1)$$

where \bar{d} is the average heliocentric distance of stars, A and B are the usual Oort constants, and C and K are given by

$$2C \equiv -\frac{\bar{u}}{r} + \frac{\partial \bar{u}}{\partial r} - \frac{1}{r} \frac{\partial \bar{v}_\phi}{\partial \phi} \quad (2)$$

¹ Department of Physics and Astronomy, University of Rochester, Rochester, NY 14627; iminchev@pas.rochester.edu, aquillen@pas.rochester.edu

² Laboratory for Laser Energetics, University of Rochester, Rochester, NY 14623; nordhaus@pas.rochester.edu

TABLE 1
SIMULATION PARAMETERS USED

Parameter	Symbol	Value
Solar neighborhood radius	r_0	1
Circular velocity at r_0	v_0	1
Radial velocity dispersion	$\sigma_u(r_0)$	0.05 v_0 or 0.18 v_0
σ_u scale length	r_σ	0.9 r_0
Disk scale length	r_ρ	0.37 r_0
Bar strength	ϵ_b	-0.012
Bar size	r_b	0.8 r_{cr}

$$2K \equiv +\frac{\bar{u}}{r} + \frac{\partial \bar{u}}{\partial r} + \frac{1}{r} \frac{\partial \bar{v}_\phi}{\partial \phi}. \quad (3)$$

Here r and ϕ are the usual polar coordinates and $v_\phi = v_0 + v$, where v_0 is the circular velocity at the Solar radius, r_0 . In this work we primarily consider a flat rotation curve (RC) (see, however §5), hence the derivatives of v_ϕ in the above equations are identical to the derivatives of v . C describes the radial shear of the velocity field and K its divergence. For an axisymmetric Galaxy we expect vanishing values for both C and K ³. Whereas C could be derived from both radial velocities and proper motions, K can only be measured from radial velocities, in which case accurate distances are also needed.

A problem with using proper motions data has been described by O&D. The authors present an effect which arises from the longitudinal variations of the mean stellar parallax caused by intrinsic density inhomogeneities. Together with the reflex of the solar motion these variations create contributions to the longitudinal proper motions which are indistinguishable from the Oort constants at $\leq 20\%$ of their amplitude. O&D corrected for the “mode-mixing” effect described above, using the latitudinal proper motions. The resulting C is found to vary approximately linearly with both color and asymmetric drift (and thus mean age) from $C \approx 0$ km/s/kpc for blue samples to $C \approx -10$ km/s/kpc for late-type stars (see Figs. 6 and 9 in O&D). Since C is related to the radial streaming of stars, we expect non-axisymmetric structure to mainly affect the low-dispersion population which would result in the opposite behavior for C . In Paper I we showed that spiral structure failed to explain the observed trend of C .

Note that the Oort constants are not constant unless they are measured in the SN. Due to nonaxisymmetries they may vary with the position in the Galaxy. Thus, the Oort constants have often been called the Oort *functions*.

3. THE SIMULATIONS

We perform 2D test-particle simulations of an initially axisymmetric exponential galactic disk. To reproduce the observed kinematics of the Milky Way, we use disk parameters consistent with observations (see Table 1). A detailed description of our disk model and simulation technique can be found in Paper I. We are interested in the variation of C with color ($B-V$), and asymmetric drift v_a . We simulate variations with color by assuming that the velocity dispersion increases from blue to red star samples. For a cold disk we start with an initial radial velocity dispersion $\sigma_u = 0.05v_0$ whereas for a hot

³ Note, however, that C and K would also be zero in the presence of nonaxisymmetric structure if the Sun happened to be located on a symmetry axis.

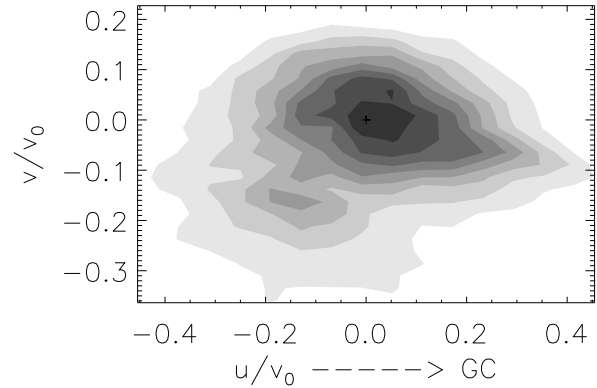


FIG. 1.— Simulated $u - v$ distribution for a Bar pattern speed $\Omega_b = 1.87\Omega_0$, Bar angle $\phi_0 = 35^\circ$ and a sample depth $d = r_0/40$. The initial velocity dispersion is $\sigma_u = 0.18v_0$ and the Bar strength is $\epsilon_b = -0.012$. Contour levels are equally spaced. The clump identified with the Hercules stream is clearly discernible in the lower left portion of the plot. This figure is in agreement with the observed $f_0(u, v)$ (Dehnen 1998; Fux 2001) and simulated distribution functions of Dehnen (2000) and Fux (2001).

disk we use $\sigma_u = 0.18v_0$. The background axisymmetric potential due to the disk and halo has the form $\Phi_0(r) = v_0^2 \log(r)$, corresponding to a flat RC.

3.1. The Bar potential

We model the nonaxisymmetric potential perturbation due to the Galactic Bar as a pure quadrupole

$$\Phi_b = A_b(\epsilon_b) \cos[2(\phi - \Omega_b t)] \times \begin{cases} \left(\frac{r_b}{r}\right)^3, & r \geq r_b \\ 2 - \left(\frac{r}{r_b}\right)^3, & r \leq r_b \end{cases} \quad (4)$$

Here $A_b(\epsilon_b)$ is the Bar’s gravitational potential amplitude, identical to the same name parameter used by Dehnen (2000); the strength is specified by $\epsilon_b = -\alpha$ from the same paper. The Bar length is $r_b = 0.8r_{cr}$ with r_{cr} the Bar corotation radius. The pattern speed, Ω_b is kept constant. We grow the Bar by linearly varying its amplitude, ϵ_b , from zero to its maximum value in four Bar rotation periods. We present our results by changing Ω_b and keeping r_0 fixed. The 2:1 outer Lindblad resonance (OLR) with the Bar is achieved when $\Omega_b/\Omega_0 = 1 + \kappa/2 \approx 1.7$, where κ is the epicyclic frequency. We examine a region of parameter space for a range of pattern speeds placing the SN just outside the OLR. For a given pattern speed one could obtain the ratio r_0/r_{OLR} through $r_0/r_{OLR} = \Omega_b/\Omega_{OLR} \approx \Omega_b/1.7$.

In contrast to Dehnen (2000) and similar to Fux (2001) and Mühlbauer & Dehnen (2003), we integrate forward in time. To allow for phase mixing to complete after the Bar reaches its maximum strength, we wait for 10 Bar rotations before we start recording the position and velocity vectors. In order to improve statistics, positions and velocities are time averaged for 10 Bar periods. After utilizing the two-fold symmetry of our galaxy we end up with $\sim 5 \times 10^5$ particles in a given simulated solar neighborhood with maximum radius $d_{max} = r_0/10$.

4. RESULTS

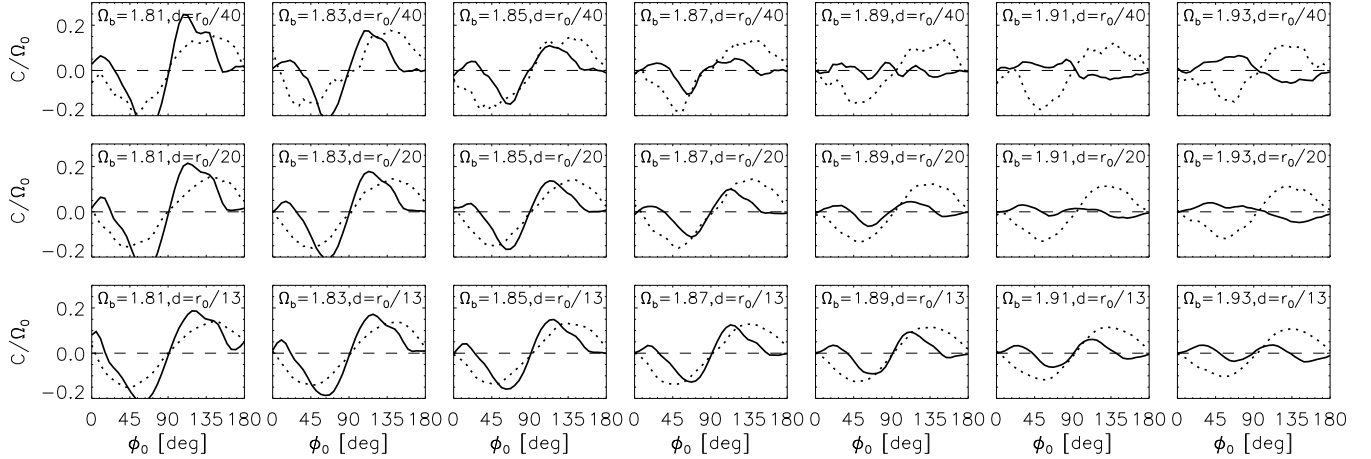


FIG. 2.— Each panel shows the variation of the Oort constant C with Bar angle ϕ_0 , for a simulation with the parameters given in Table 1 and a particular Bar pattern speed, Ω_b , and a mean sample depth, \bar{d} . Solid and dotted lines correspond to cold- and hot-disk values, respectively. Columns from left to right, show an increasing Ω_b in units of Ω_0 . Note that the OLR is at $\Omega_{OLR} \approx 1.7$. Different rows present results from samples with different mean heliocentric distance, \bar{d} . Good matches to the observed trend in C (vanishing value for the cold disk and a large negative for the hot one) are achieved for $20^\circ \leq \phi_0 \leq 45^\circ$ and $1.83 \leq \Omega_b/\Omega_0 \leq 1.91$.

First we show that we can reproduce the results of Dehnen and Fux for the Hercules stream. We present a simulated $u - v$ velocity distribution for $\Omega_b = 1.87\Omega_0$, $\phi_0 = 35^\circ$, and a sample depth $\bar{d} = r_0/40$ in fig. 1. The initial velocity dispersion is $\sigma_u = 0.18v_0$. This plot is indeed in very good agreement with previous test-particle (Dehnen 2000; Fux 2001) and N-body (Fux 2001) simulations.

By a quantitative comparison of the observed with the simulated distributions, Dehnen (2000) deduced the Milky Way Bar pattern speed to be $\Omega_b/\Omega_0 = 1.85 \pm 0.15$. In this calculation only the local velocity field, i.e., the observed $u - v$ distribution, was taken into account. Now, if one could also relate the dynamical effect of the Bar to the derivatives of the velocities, an additional constraint on Bar parameters would be provided. Since the gradients of u and v are hard to measure directly, one needs an indirect way of achieving this task. The obvious candidates, as anticipated, are the Oort constants C and K . Oort's K , however, is hard to measure as mentioned above; hence only C , as estimated by O&D, will be employed here. By Fourier expansion of eqs. 1 (see Paper I for details) we estimate C from our numerically simulated velocity distributions for the initially cold and hot disks.

4.1. Variation of C with Bar pattern speed and orientation

In Fig. 3.1 we present our results for C as a function of the Bar angle, ϕ_0 (the angle by which the Sun's azimuth lags the Bar's major axis). Each column shows a simulation with a different pattern speed, indicated in each plot. Rows from top to bottom show C as calculated from samples at average heliocentric distances corresponding to $\bar{d} = 200$, $\bar{d} = 400$, and $\bar{d} = 600$ pc, for a Solar radius $r_0 = 7.8$ kpc. Solid and dotted lines represent the results for cold and hot disks, respectively. The dashed lines indicates $C = 0$. C is presented in units of $\Omega_0 = v_0/r_0$. To make the discussion less cumbersome, we

write C_h and C_c to refer to the values for C as estimated from the hot and cold disks, respectively.

C_h (dotted lines in Fig. 3.1) varies with galactic azimuth as $C_h(\phi_0) \sim \sin(2\phi_0)$ for all of the Ω_b values considered. On the other hand, the cold disk values (solid line) exhibit different variations, depending on Ω_b or equivalently, on the ratio r_0/r_{OLR} . Closer to the OLR (left columns of Fig. 3.1), $C_c(\phi_0)$ approaches the functional behavior of $C_h(\phi_0)$. Away from the OLR $C_c(\phi_0)$ is shifted by 90° compared to $C_h(\phi_0)$. While both cold and hot disks yield in increase in the amplitude of $C(\phi_0)$ as the pattern speed nears the OLR, the effect on the $C_c(\phi_0)$ is much stronger. This is consistent with our expectation that the cold disk is affected more by the Bar, especially near the OLR. While close to the OLR $|C_h(\phi_0)| < |C_c(\phi_0)|$, we observe the opposite behavior away from it. This could be explained by the results of Mühlbauer & Dehnen (2003), where they find that high velocity dispersion stars tend to shift the “effective resonance” radially outwards.

According to O&D's “mode-mixing” corrected value, $C \approx 0$ for the cold sample and decreases to about -10 km/s for the hot population. Hence we look for locations in Fig. 3.1 complying with this requirement. In the transition region, $1.83 \leq \Omega_b/\Omega_0 \leq 1.91$, where the function $C_c(\phi_0)$ transforms into its negative, there are specific angles which provide good matches for the observations, i.e., $C_c(\phi_0) \approx 0$ while $C_h(\phi_0)$ is significantly negative. We performed simulations with different pattern speeds in the range $1.7 \leq \Omega_b/\Omega_0 \leq 2.5$. It was found that only in the transition region in Fig. 3.1 could one achieve a satisfactory match to the observations. Although the left- and right-most columns are nearly consistent with our requirement on C , we reject these values of Ω_b for the following reason. O&D estimated a large negative C from both the reddest main-sequence stars, which are nearby, and the more distant red giants. This is inconsistent with the largest mean sample depth shown in Fig. 3.1 with $\Omega_b = 1.81, 1.93$. We conclude that the

Bar pattern speed must lie in the range

$$\Omega_b/\Omega_0 = 1.87 \pm 0.04. \quad (5)$$

The Bar angle with respect to the Sun has been proposed, as derived from IR photometry, to lie in the range $15^\circ - 45^\circ$ with the Sun lagging the Bar major axis, whereas Dehnen (2000) found that the Bar reproduced the u -anomaly for $10^\circ \leq \phi_0 \leq 70^\circ$. Examining Fig. 3.1, we find that our requirements on C result in constraining the Bar angle in the range $20^\circ \leq \phi_0 \leq 45^\circ$, depending on Ω_b . This result for the dependence of pattern speed on Bar angle is in a very good agreement with Fig. 10 by Dehnen (2000) which shows a linear increase of the derived Ω_b/Ω_0 as a function of ϕ_0 . This is remarkable since Dehnen (2000) obtained his results in a completely different way than our method here.

4.2. The effect of the Bar on A and B

The Oort constants A and B were found to also be affected by the Bar, although to a much smaller extent. One could estimate the Bar-induced errors as $\Delta A \equiv A - A_{\text{axi}}$ and $\Delta B \equiv B - B_{\text{axi}}$. Here A_{axi} , B_{axi} are the resulting axisymmetric values when simulations excluding the Bar perturbation are performed. Note that we require a different simulation with each of the initial radial velocity dispersions used in order to estimate the asymmetric drift induced errors. We found that for the cold disk the Bar causes $\Delta A = 3.5 \pm 0.7$ and $\Delta B = 3 \pm 0.6$ km/s/kpc, while the hot disk yielded $\Delta A = 0.5 \pm 1.5$ and $\Delta B = 0 \pm 1$ km/s/kpc. These values are calculated for $r_0 = 7.8$ kpc and $v_0 = 220$ km/s. Despite the Bar's effect on C , the hot population does provide better measurements for A and B .

O&D found an approximately linear variation of A and B with color with A increasing and B decreasing. The Bar induced errors presented here match the observed trend of B but have the opposite one for A . It is possible that local spiral structure is responsible for this discrepancy.

5. CONCLUSION

We have shown that the Galactic Bar can account for a trend seen in measurements of Oort's C , namely a more negative C -value with increasing velocity dispersion. This trend is difficult to explain with other dynamical models (e.g., Paper I). By requiring that the Bar model accounts for this trend in C , we have improved the measurement of the Bar pattern speed, find-

ing $\Omega_b/\Omega_0 = 1.87 \pm 0.04$. In addition, the Bar angle is found to be in the range $20^\circ \leq \phi_0 \leq 45^\circ$. Our result for Ω_b lies well within the estimate by Dehnen (2000) and that by Debattista et al. (2002), based on OH/IR star kinematics. This study provides an improvement on the measurement of the Bar pattern speed by a factor of ~ 4 compared to previous work (Dehnen 2000). The improved constraints on Bar parameters should be tested by, and will benefit, future studies of the Bar structure in the Galactic center region, that will become possible with future radial velocity and proper motion studies (e.g., BRAVA, Rich et al. 2007).

In addition to a flat RC we have also considered a power law initial tangential velocity $v_\phi = v_0(r/r_0)^\beta$ with $\beta = 0.1, -0.1$ corresponding to a rising and a declining RC, respectively. We found that for $\beta = 0.1$ no additional error in Ω_b is introduced. However, for $\beta = -0.1$ we estimated $\Omega_b/\Omega_0 = 1.85 \pm 0.06$. From Fig. 3.1 we see that the main source of error in the Bar pattern speed is due to the uncertainty in the Bar angle. A recent work by Rattenbury et al. (2007) used OGLE-II microlensing observations of red clump giants in the Galactic bulge, to estimate a bar angle of $24^\circ - 27^\circ$. Using this as an additional constraint we obtain $\Omega_b/\Omega_0 = 1.84 \pm 0.01$.

While we account for the trend of increasingly negative C with increasing velocity dispersion, we fail to reproduce the size of the C -value measured by O&D. The most negative value we predict is about -6 while they measure -10 km/s/kpc. We discuss possible reasons for this discrepancy: (i) we expect that the magnitude of C is related to the fraction of SN stars composing the Hercules stream. It is possible that during its formation the Bar changed its pattern speed forcing more stars to be trapped in the 2:1 OLR, thus increasing this fraction. This would give rise to a more negative C from hot stars, while leaving the cold population unaffected; (ii) the numerical model here uses a distance limited sample. Modeling a stellar population with a magnitude limited sample is more appropriate to compare to the observed measurements. (iii) O&D's "mode-mixing" correction is only valid if the Sun's motion in the z -direction were assumed constant. This is invalidated if, for example, a local Galactic warp were present.

Support for this work was in part provided by NSF grant ASST-0406823, and NASA grant No. NNG04GM12G issued through the Origins of Solar Systems Program.

REFERENCES

Bensby, T., Oey, M. S., Feltzing, S., & Gustafsson, B. 2007, ApJ, 655, L89

Blitz, L., & Spergel, D. N. 1991, ApJ, 379, 631

Debattista, V. P., Gerhard, O., & Sevenster, M. N. 2002, MNRAS, 334, 355

Dehnen, W. 1998, AJ, 115, 2384

Dehnen, W. 1999, ApJ, 524, L35

Dehnen, W. 2000, AJ, 119, 800

Famaey, B., Jorissen, A., Luri, X., Mayor, M., Udry, S., Dejonghe, H., & Turon, C. 2005, A&A, 430, 165

Fux, R. 2001, A&A, 373, 511

Kuijken, K., & Tremaine, S. 1991, in Sundelius B., ed., Dynamics of Disc Galaxies, Gteborg Univ. Press, p. 71

Minchev, I., & Quillen, A. C. 2006, MNRAS, 368, 623

Minchev, I., & Quillen, A. C. 2007, MNRAS, 377, 1163 (Paper I)

Mühlbauer, G., & Dehnen, W. 2003, A&A, 401, 975

Olling, R. P., & Dehnen, W. 2003, ApJ, 599, 275 (O&D)

Rattenbury, N. J., Mao, S., Sumi, T., & Smith, M. C. 2007, ArXiv e-prints, 704, arXiv:0704.1614

Rich, R. M., Reitzel, D. B., Howard, C. D., & Zhao, H. 2007, ApJ, 658, L29

Torra, J., Fernández, D., & Figueras, F. 2000, A&A, 359, 82

Weinberg, M. D. 1992, ApJ, 384, 81

NEW CONSTRAINTS ON THE GALACTIC BAR

I. MINCHEV¹, J. NORDHAUS^{1,2} AND A. C. QUILLEN¹

Draft version December 11, 2007

ABSTRACT

Previous work has related the Galactic Bar to structure in the local stellar velocity distribution. Here we show that the Bar also influences the spatial gradients of the velocity vector via the Oort constants. By numerical integration of test-particles we simulate measurements of the Oort C value in a gravitational potential including the Galactic Bar. We account for the observed trend that C is increasingly negative for stars with higher velocity dispersion. By comparing measurements of C with our simulations we improve on previous models of the Bar, estimating that the Bar pattern speed is $\Omega_b/\Omega_0 = 1.87 \pm 0.04$, where Ω_0 is the local circular frequency, and the Bar angle lies within $20^\circ \leq \phi_0 \leq 45^\circ$. We find that the Galactic Bar affects measurements of the Oort constants A and B less than ~ 2 km/s/kpc for the hot stars.

Subject headings:

1. INTRODUCTION

The Galaxy is often modeled as an axisymmetric disk. With the ever increasing proper motion and radial velocity data, it is now apparent that nonaxisymmetric effects cannot be neglected (nonzero Oort constant C , Olling & Dehnen 2003, hereafter O&D; nonzero vertex deviation, Famaey et al. 2005; asymmetries in the local velocity distribution of stars, Dehnen 1998). It is still not clear, however, what the exact nature of the perturbing agent(s) in the Solar neighborhood (SN) is(are). Possible candidates are spiral density waves, a central Bar, and a triaxial halo.

Due to our position in the Galactic disk, the properties of the Milky Way Bar are hard to observe directly. Hence its parameters, such as orientation and pattern speed, have only been inferred indirectly from observations of the inner Galaxy (e.g., Blitz & Spergel 1991; Weinberg 1992).

However, the Bar has also been found to affect the local velocity distribution of stars. *HIPPARCOS* data revealed more clearly a stream of old disk stars with an asymmetric drift of about 45 km/s and a radial velocity $u < 0$, with u and v positive toward the Galactic center and in the direction of Galactic rotation, respectively. This agglomeration of stars has been dubbed the “Hercules” stream or the “ u -anomaly”. The numerical work of Dehnen (1999, 2000) and Fux (2001) has shown that this stream can be explained as the effect of the Milky Way Bar if the Sun is placed just outside the 2:1 Outer Lindblad Resonance (OLR). Using high-resolution spectra of nearby F and G dwarf stars, Bensby et al. (2007) have investigated the detailed abundance and age structure of the Hercules stream. Since this stream is composed of stars of different ages and metallicities pertinent to both thin and thick disks, they concluded that a dynamical effect, such as the influence of the Bar, is a more likely explanation than a dispersed cluster.

¹ Department of Physics and Astronomy, University of Rochester, Rochester, NY 14627; iminchev@pas.rochester.edu, aquillen@pas.rochester.edu

² Laboratory for Laser Energetics, University of Rochester, Rochester, NY 14623; nordhaus@pas.rochester.edu

Assuming the Galactic Bar affects the shape of the distribution function of the old stellar population in the SN, an additional constraint on the Bar can be provided by considering the values derived for the Oort constant C . In other words, in addition to relating the dynamical influence of the Bar to the local velocity field, C provides a link to the gradients of the velocities as well. The study of O&D not only measured a non-zero C , implying the presence of non-circular motion in the SN, but also found that C is more negative for older and redder stars with a larger velocity dispersion. This is surprising as a hotter stellar population is expected to have averaged properties more nearly axisymmetric and hence, a reduced value of $|C|$ (e.g., Minchev & Quillen 2007; hereafter Paper I).

It is the aim of this letter to show it is indeed possible to explain the observationally deduced trend for C (O&D) by modeling the Milky Way as an exponential disk perturbed by a central Bar. By performing this exercise, we provide additional constraints on the Bar’s pattern speed. Models for the structure in the bulge of our galaxy are difficult to constrain because of the large numbers of degrees of freedom in Bar models. Thus future studies of structure in the Galactic Center will benefit from tighter constraints on the parameters describing the Bar, such as its pattern speed and angle with respect to the Sun.

2. THE OORT CONSTANTS

We can linearize the local velocity field (e.g., Paper I) about the LSR and write the mean radial velocity \bar{v}_d and longitudinal proper motion $\bar{\mu}_l$ as functions of the Galactic longitude l as

$$\frac{\bar{v}_d}{\bar{d}} = K + A \sin(2l) + C \cos(2l) \quad (1)$$

$$\bar{\mu}_l = B + A \cos(2l) - C \sin(2l)$$

where \bar{d} is the average heliocentric distance of stars, A and B are the usual Oort constants, and C and K are given by

$$2C \equiv -\frac{\bar{u}}{r} + \frac{\partial \bar{u}}{\partial r} - \frac{1}{r} \frac{\partial \bar{v}_\phi}{\partial \phi} \quad (2)$$

$$2K \equiv +\frac{\bar{u}}{r} + \frac{\partial \bar{u}}{\partial r} + \frac{1}{r} \frac{\partial \bar{v}_\phi}{\partial \phi}. \quad (3)$$

TABLE 1
SIMULATION PARAMETERS USED

Parameter	Symbol	Value
Solar neighborhood radius	r_0	1
Circular velocity at r_0	v_0	1
Radial velocity dispersion	$\sigma_u(r_0)$	0.05 v_0 or 0.18 v_0
σ_u scale length	r_σ	0.9 r_0
Disk scale length	r_ρ	0.37 r_0
Bar strength	ϵ_b	-0.012
Bar size	r_b	0.8 r_{cr}

Here r and ϕ are the usual polar coordinates and $v_\phi = v_0 + v$, where v_0 is the circular velocity at the Solar radius, r_0 . In this work we primarily consider a flat rotation curve (RC) (see, however §5), hence the derivatives of v_ϕ in the above equations are identical to the derivatives of v . C describes the radial shear of the velocity field and K its divergence. For an axisymmetric Galaxy we expect vanishing values for both C and K ³. Whereas C could be derived from both radial velocities and proper motions, K can only be measured from radial velocities, in which case accurate distances are also needed.

A problem with using proper motions data has been described by O&D. The authors present an effect which arises from the longitudinal variations of the mean stellar parallax caused by intrinsic density inhomogeneities. Together with the reflex of the solar motion these variations create contributions to the longitudinal proper motions which are indistinguishable from the Oort constants at $\leq 20\%$ of their amplitude. O&D corrected for the “mode-mixing” effect described above, using the latitudinal proper motions. The resulting C is found to vary approximately linearly with both color and asymmetric drift (and thus mean age) from $C \approx 0$ km/s/kpc for blue samples to $C \approx -10$ km/s/kpc for late-type stars (see Figs. 6 and 9 in O&D). Since C is related to the radial streaming of stars, we expect non-axisymmetric structure to mainly affect the low-dispersion population which would result in the opposite behavior for C . In Paper I we showed that spiral structure failed to explain the observed trend of C .

Note that the Oort constants are not constant unless they are measured in the SN. Due to nonaxisymmetries they may vary with the position in the Galaxy. Thus, the Oort constants have often been called the Oort *functions*.

3. THE SIMULATIONS

We perform 2D test-particle simulations of an initially axisymmetric exponential galactic disk. To reproduce the observed kinematics of the Milky Way, we use disk parameters consistent with observations (see Table 1). A detailed description of our disk model and simulation technique can be found in Paper I. We are interested in the variation of C with color ($B-V$), and asymmetric drift v_a . We simulate variations with color by assuming that the velocity dispersion increases from blue to red star samples. For a cold disk we start with an initial radial velocity dispersion $\sigma_u = 0.05v_0$ whereas for a hot disk we use $\sigma_u = 0.18v_0$. The background axisymmetric

³ Note, however, that C and K would also be zero in the presence of nonaxisymmetric structure if the Sun happened to be located on a symmetry axis.

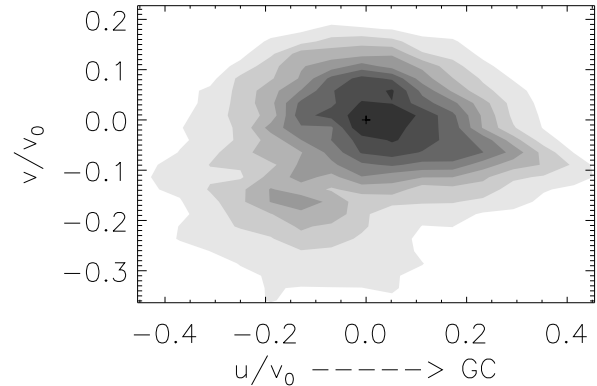


FIG. 1.— Simulated $u - v$ distribution for a Bar pattern speed $\Omega_b = 1.87v_0$, Bar angle $\phi_0 = 35^\circ$ and a sample depth $d = r_0/40$. The initial velocity dispersion is $\sigma_u = 0.18v_0$ and the Bar strength is $\epsilon_b = -0.012$. Contour levels are equally spaced. The clump identified with the Hercules stream is clearly discernible in the lower left portion of the plot. This figure is in agreement with the observed $f_0(u, v)$ (Dehnen 1998; Fux 2001) and simulated distribution functions of Dehnen (2000) and Fux (2001).

potential due to the disk and halo has the form $\Phi_0(r) = v_0^2 \log(r)$, corresponding to a flat RC.

3.1. The Bar potential

We model the nonaxisymmetric potential perturbation due to the Galactic Bar as a pure quadrupole

$$\Phi_b = A_b(\epsilon_b) \cos[2(\phi - \Omega_b t)] \times \begin{cases} \left(\frac{r_b}{r}\right)^3, & r \geq r_b \\ 2 - \left(\frac{r}{r_b}\right)^3, & r \leq r_b \end{cases} \quad (4)$$

Here $A_b(\epsilon_b)$ is the Bar’s gravitational potential amplitude, identical to the same name parameter used by Dehnen (2000); the strength is specified by $\epsilon_b = -\alpha$ from the same paper. The Bar length is $r_b = 0.8r_{cr}$ with r_{cr} the Bar corotation radius. The pattern speed, Ω_b is kept constant. We grow the Bar by linearly varying its amplitude, ϵ_b , from zero to its maximum value in four Bar rotation periods. We present our results by changing Ω_b and keeping r_0 fixed. The 2:1 outer Lindblad resonance (OLR) with the Bar is achieved when $\Omega_b/\Omega_0 = 1 + \kappa/2 \approx 1.7$, where κ is the epicyclic frequency. We examine a region of parameter space for a range of pattern speeds placing the SN just outside the OLR. For a given pattern speed one could obtain the ratio r_0/r_{OLR} through $r_0/r_{OLR} = \Omega_b/\Omega_{OLR} \approx \Omega_b/1.7$.

In contrast to Dehnen (2000) and similar to Fux (2001) and Mühlbauer & Dehnen (2003), we integrate forward in time. To allow for phase mixing to complete after the Bar reaches its maximum strength, we wait for 10 Bar rotations before we start recording the position and velocity vectors. In order to improve statistics, positions and velocities are time averaged for 10 Bar periods. After utilizing the two-fold symmetry of our galaxy we end up with $\sim 5 \times 10^5$ particles in a given simulated solar neighborhood with maximum radius $d_{max} = r_0/10$.

4. RESULTS

First we show that we can reproduce the results of Dehnen and Fux for the Hercules stream. We present a

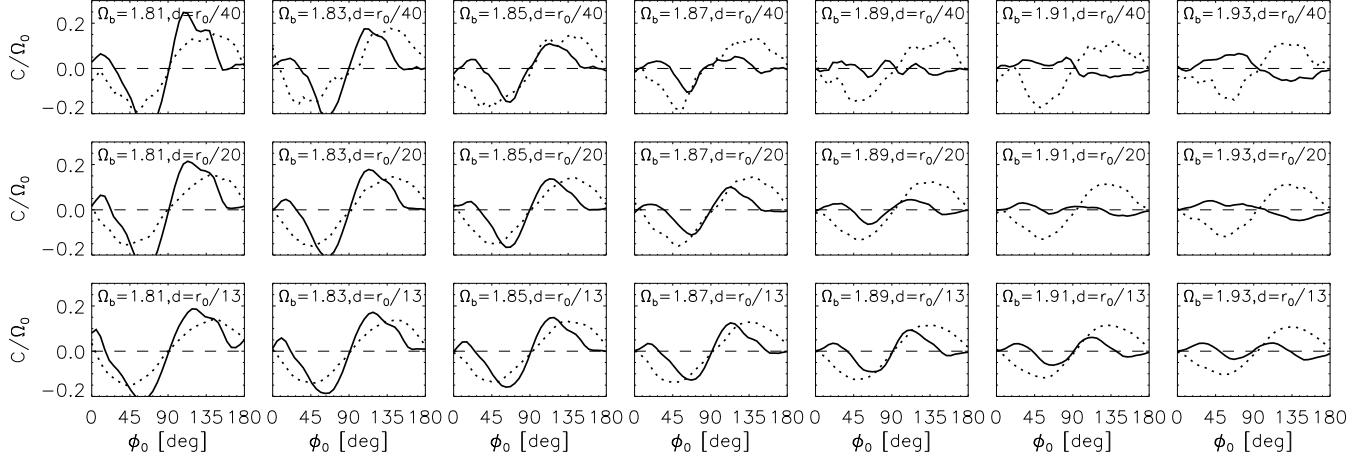


FIG. 2.— Each panel shows the variation of the Oort constant C with Bar angle ϕ_0 , for a simulation with the parameters given in Table 1 and a particular Bar pattern speed, Ω_b , and a mean sample depth, \bar{d} . Solid and dotted lines correspond to cold- and hot-disk values, respectively. Columns from left to right, show an increasing Ω_b in units of Ω_0 . Note that the OLR is at $\Omega_{OLR} \approx 1.7$. Different rows present results from samples with different mean heliocentric distance, \bar{d} . Good matches to the observed trend in C (vanishing value for the cold disk and a large negative for the hot one) are achieved for $20^\circ \leq \phi_0 \leq 45^\circ$ and $1.83 \leq \Omega_b/\Omega_0 \leq 1.91$.

simulated $u - v$ velocity distribution for $\Omega_b = 1.87\Omega_0$, $\phi_0 = 35^\circ$, and a sample depth $\bar{d} = r_0/40$ in fig. 1. The initial velocity dispersion is $\sigma_u = 0.18v_0$. This plot is indeed in very good agreement with previous test-particle (Dehnen 2000; Fux 2001) and N-body (Fux 2001) simulations.

By a quantitative comparison of the observed with the simulated distributions, Dehnen (2000) deduced the Milky Way Bar pattern speed to be $\Omega_b/\Omega_0 = 1.85 \pm 0.15$. In this calculation only the local velocity field, i.e., the observed $u - v$ distribution, was taken into account. Now, if one could also relate the dynamical effect of the Bar to the derivatives of the velocities, an additional constraint on Bar parameters would be provided. Since the gradients of u and v are hard to measure directly, one needs an indirect way of achieving this task. The obvious candidates, as anticipated, are the Oort constants C and K . Oort's K , however, is hard to measure as mentioned above; hence only C , as estimated by O&D, will be employed here. By Fourier expansion of eqs. 1 (see Paper I for details) we estimate C from our numerically simulated velocity distributions for the initially cold and hot disks.

4.1. Variation of C with Bar pattern speed and orientation

In Fig. 3.1 we present our results for C as a function of the Bar angle, ϕ_0 (the angle by which the Sun's azimuth lags the Bar's major axis). Each column shows a simulation with a different pattern speed, indicated in each plot. Rows from top to bottom show C as calculated from samples at average heliocentric distances corresponding to $\bar{d} = 200$, $\bar{d} = 400$, and $\bar{d} = 600$ pc, for a Solar radius $r_0 = 7.8$ kpc. Solid and dotted lines represent the results for cold and hot disks, respectively. The dashed lines indicates $C = 0$. C is presented in units of $\Omega_0 = v_0/r_0$. To make the discussion less cumbersome, we write C_h and C_c to refer to the values for C as estimated from the hot and cold disks, respectively.

C_h (dotted lines in Fig. 3.1) varies with galactic azimuth as $C_h(\phi_0) \sim \sin(2\phi_0)$ for all of the Ω_b values considered. On the other hand, the cold disk values (solid line) exhibit different variations, depending on Ω_b or equivalently, on the ratio r_0/r_{OLR} . Closer to the OLR (left columns of Fig. 3.1), $C_c(\phi_0)$ approaches the functional behavior of $C_h(\phi_0)$. Away from the OLR $C_c(\phi_0)$ is shifted by 90° compared to $C_h(\phi_0)$. While both cold and hot disks yield in increase in the amplitude of $C(\phi_0)$ as the pattern speed nears the OLR, the effect on the $C_c(\phi_0)$ is much stronger. This is consistent with our expectation that the cold disk is affected more by the Bar, especially near the OLR. While close to the OLR $|C_h(\phi_0)| < |C_c(\phi_0)|$, we observe the opposite behavior away from it. This could be explained by the results of Mühlbauer & Dehnen (2003), where they find that high velocity dispersion stars tend to shift the “effective resonance” radially outwards.

According to O&D's “mode-mixing” corrected value, $C \approx 0$ for the cold sample and decreases to about -10 km/s for the hot population. Hence we look for locations in Fig. 3.1 complying with this requirement. In the transition region, $1.83 \leq \Omega_b/\Omega_0 \leq 1.91$, where the function $C_c(\phi_0)$ transforms into its negative, there are specific angles which provide good matches for the observations, i.e., $C_c(\phi_0) \approx 0$ while $C_h(\phi_0)$ is significantly negative. We performed simulations with different pattern speeds in the range $1.7 \leq \Omega_b/\Omega_0 \leq 2.5$. It was found that only in the transition region in Fig. 3.1 could one achieve a satisfactory match to the observations. Although the left- and right-most columns are nearly consistent with our requirement on C , we reject these values of Ω_b for the following reason. O&D estimated a large negative C from both the reddest main-sequence stars, which are nearby, and the more distant red giants. This is inconsistent with the largest mean sample depth shown in Fig. 3.1 with $\Omega_b = 1.81, 1.93$. We conclude that the Bar pattern speed must lie in the range

$$\Omega_b/\Omega_0 = 1.87 \pm 0.04. \quad (5)$$

The Bar angle with respect to the Sun has been proposed, as derived from IR photometry, to lie in the range $15^\circ - 45^\circ$ with the Sun lagging the Bar major axis, whereas Dehnen (2000) found that the Bar reproduced the u -anomaly for $10^\circ \leq \phi_0 \leq 70^\circ$. Examining Fig. 3.1, we find that our requirements on C result in constraining the Bar angle in the range $20^\circ \leq \phi_0 \leq 45^\circ$, depending on Ω_b . This result for the dependence of pattern speed on Bar angle is in a very good agreement with Fig. 10 by Dehnen (2000) which shows a linear increase of the derived Ω_b/Ω_0 as a function of ϕ_0 . This is remarkable since Dehnen (2000) obtained his results in a completely different way than our method here.

4.2. The effect of the Bar on A and B

The Oort constants A and B were found to also be affected by the Bar, although to a much smaller extent. One could estimate the Bar-induced errors as $\Delta A \equiv A - A_{\text{axi}}$ and $\Delta B \equiv B - B_{\text{axi}}$. Here A_{axi} , B_{axi} are the resulting axisymmetric values when simulations excluding the Bar perturbation are performed. Note that we require a different simulation with each of the initial radial velocity dispersions used in order to estimate the asymmetric drift induced errors. We found that for the cold disk the Bar causes $\Delta A = 3.5 \pm 0.7$ and $\Delta B = 3 \pm 0.6$ km/s/kpc, while the hot disk yielded $\Delta A = 0.5 \pm 1.5$ and $\Delta B = 0 \pm 1$ km/s/kpc. These values are calculated for $r_0 = 7.8$ kpc and $v_0 = 220$ km/s. Despite the Bar's effect on C , the hot population does provide better measurements for A and B .

O&D found an approximately linear variation of A and B with color with A increasing and B decreasing. The Bar induced errors presented here match the observed trend of B but have the opposite one for A . It is possible that local spiral structure is responsible for this discrepancy.

5. CONCLUSION

We have shown that the Galactic Bar can account for a trend seen in measurements of Oort's C , namely a more negative C -value with increasing velocity dispersion. This trend is difficult to explain with other dynamical models (e.g., Paper I). By requiring that the Bar model accounts for this trend in C , we have improved the measurement of the Bar pattern speed, finding $\Omega_b/\Omega_0 = 1.87 \pm 0.04$. In addition, the Bar angle is found to be in the range $20^\circ \leq \phi_0 \leq 45^\circ$. Our result

for Ω_b lies well within the estimate by Dehnen (2000) and that by Debattista et al. (2002), based on OH/IR star kinematics. This study provides an improvement on the measurement of the Bar pattern speed by a factor of ~ 4 compared to previous work (Dehnen 2000). The improved constraints on Bar parameters should be tested by, and will benefit, future studies of the Bar structure in the Galactic center region, that will become possible with future radial velocity and proper motion studies (e.g., BRAVA, Rich et al. 2007).

In addition to a flat RC we have also considered a power law initial tangential velocity $v_\phi = v_0(r/r_0)^\beta$ with $\beta = 0.1, -0.1$ corresponding to a rising and a declining RC, respectively. We found that for $\beta = 0.1$ no additional error in Ω_b is introduced. However, for $\beta = -0.1$ we estimated $\Omega_b/\Omega_0 = 1.85 \pm 0.06$. From Fig. 3.1 we see that the main source of error in the Bar pattern speed is due to the uncertainty in the Bar angle. A recent work by Rattenbury et al. (2007) used OGLE-II microlensing observations of red clump giants in the Galactic bulge, to estimate a bar angle of $24^\circ - 27^\circ$. Using this as an additional constraint we obtain $\Omega_b/\Omega_0 = 1.84 \pm 0.01$.

While we account for the trend of increasingly negative C with increasing velocity dispersion, we fail to reproduce the size of the C -value measured by O&D. The most negative value we predict is about -6 while they measure -10 km/s/kpc. We discuss possible reasons for this discrepancy: (i) we expect that the magnitude of C is related to the fraction of SN stars composing the Hercules stream. It is possible that during its formation the Bar changed its pattern speed forcing more stars to be trapped in the 2:1 OLR, thus increasing this fraction. This would give rise to a more negative C from hot stars, while leaving the cold population unaffected; (ii) the numerical model here uses a distance limited sample. Modeling a stellar population with a magnitude limited sample is more appropriate to compare to the observed measurements. (iii) O&D's "mode-mixing" correction is only valid if the Sun's motion in the z -direction were assumed constant. This is invalidated if, for example, a local Galactic warp were present.

Support for this work was in part provided by NSF grant ASST-0406823, and NASA grant No. NNG04GM12G issued through the Origins of Solar Systems Program.

REFERENCES

Bensby, T., Oey, M. S., Feltzing, S., & Gustafsson, B. 2007, ApJ, 655, L89
 Blitz, L., & Spergel, D. N. 1991, ApJ, 379, 631
 Debattista, V. P., Gerhard, O., & Sevenster, M. N. 2002, MNRAS, 334, 355
 Dehnen, W. 1998, AJ, 115, 2384
 Dehnen, W. 1999, ApJ, 524, L35
 Dehnen, W. 2000, AJ, 119, 800
 Famaey, B., Jorissen, A., Luri, X., Mayor, M., Udry, S., Dejonghe, H., & Turon, C. 2005, A&A, 430, 165
 Fux, R. 2001, A&A, 373, 511
 Kuijken, K., & Tremaine, S. 1991, in Sundelius B., ed., Dynamics of Disc Galaxies, Gteborg Univ. Press, p. 71
 Minchev, I., & Quillen, A. C. 2006, MNRAS, 368, 623
 Minchev, I., & Quillen, A. C. 2007, MNRAS, 377, 1163 (Paper I)
 Mühlbauer, G., & Dehnen, W. 2003, A&A, 401, 975
 Olling, R. P., & Dehnen, W. 2003, ApJ, 599, 275 (O&D)
 Rattenbury, N. J., Mao, S., Sumi, T., & Smith, M. C. 2007, ArXiv e-prints, 704, arXiv:0704.1614
 Rich, R. M., Reitzel, D. B., Howard, C. D., & Zhao, H. 2007, ApJ, 658, L29
 Torra, J., Fernández, D., & Figueras, F. 2000, A&A, 359, 82
 Weinberg, M. D. 1992, ApJ, 384, 81